Raman Spectroscopic Studies and Ab Initio Calculations on Conformational Isomerism of 1-Butyl-3-methylimidazolium Bis-(trifluoromethanesulfonyl)amide Solvated to a Lithium Ion in I...

ARTICLE *in* THE JOURNAL OF PHYSICAL CHEMISTRY B · MAY 2010

Impact Factor: 3.3 · DOI: 10.1021/jp100898h · Source: PubMed

Raman Spectroscopic Studies and Ab Initio Calculations on Conformational Isomerism of 1-Butyl-3-methylimidazolium Bis-(trifluoromethanesulfonyl)amide Solvated to a Lithium Ion in Ionic Liquids: Effects of the Second Solvation Sphere of the Lithium Ion

Yasuhiro Umebayashi,*,† Shuto Mori,† Kenta Fujii,‡ Seiji Tsuzuki,*,§ Shiro Seki,⊥ Kikuko Hayamizu,§ and Shin-ichi Ishiguro†

Department of Chemistry, Faculty of Science, Kyushu University, Hakozaki, Higashi-ku, Fukuoka 812-8581, Japan, Department of Chemistry and Applied Chemistry, Faculty of Science and Engineering, Saga University, Honjo-machi, Saga 840-8502, Japan, National Institute of Advanced Industrial Science and Technology, Tsukuba Center 5, Tsukuba, Ibaraki 305-8565, Japan, and Materials Science Research Laboratory, Central Research Institute of Electric Power Industry, 2-11-1, Iwado-kita, Komae, Tokyo 201-8511, Japan

Received: January 30, 2010; Revised Manuscript Received: March 14, 2010

Raman spectra of the ionic liquid, 1-butyl-3-methylimidazolium bis-(trifluoromethanesulfonyl)amide [C_4mIm][TFSA] containing a LiTFSA salt were measured for the lithium salt mole fractions $x_{Li} = 0.000$, 0.053, 0.106, and 0.171 in the temperature range of 273−350 K. The lithium ion solvation number of 2 at ambient temperature is kept constant in higher temperatures examined in this study. Thermodynamic quantities, such as Gibbs free energy, $\Delta_{iso}G^0$; enthalpy, $\Delta_{iso}H^0$; and entropy, $\Delta_{iso}S^0$, for conformational isomerism of $TFSA^-$ from trans to cis isomers in the neat ionic liquid and also in the first solvation sphere of the lithium ion were successfully evaluated for the first time. In the neat ionic liquid, the thermodynamics quantities indicates that the trans isomer is slightly stabilized by enthalpy, though the enthalpic advantage is reduced by entropy to yield nearly equal Gibbs free energy. For the $TFSA^-$ in the first solvation sphere of the lithium ion, the $\Delta_{iso}G^0$, $\Delta_{iso}H^0$, and $T\Delta_{iso}S^0$ were obtained at 298 K to be −4, −9.4, and −5 kJ mol^{-1}, respectively, and the cis isomer is clearly more favored due to the larger enthalpy relative to that for the neat ionic liquid. However, gas phase quantum calculations for the lithium ion solvated clusters of $[Li(TFSA)_2]^-$ were reported to be opposite to the experimental isomerization enthalpy. In this study, additional MP2 level ab initio calculations were carried out for the lithium ion solvated clusters with a countercation of 1-ethyl-3-methylimidazolium [C_2mIm] in gas phase to yield the energy difference of −8.8 kJ mol^{-1} from [C_2mIm][Li(*trans*-$TFSA)_2$] to [C_2mIm][Li(*cis*-$TFSA)_2$]. The ab initio calculations revealed the important roles of the surrounding imidazolium cation as the second solvation sphere of the lithium ion and agree with the Raman experimental fact that the *cis*-$TFSA^-$ solvated to the lithium ion is more stabilized relative to the trans with relatively large enthalpy.

Introduction

Room-temperature ionic liquids are strongly expected to be new materials for high-energy density electrochemical devices with high safety because of their favorable properties, such as a wide electrochemical window, relatively high chemical and thermal stability, and negligible vapor pressure (thus, practical nonflammability).[1] In particular, lithium batteries[2] using ionic liquids are one of the most promising ubiquitous electric storage devices.[3−5] For this purpose, bis-(trifluoromethanesulfonyl)amide ($TFSA^-$)-based ionic liquids with various cations have been well-investigated.[6−8] To achieve higher performance of lithium batteries, particularly in terms of the current density, it is important to clarify the lithium ion transport properties in the TFSA-based ionic liquids. Thus, self-diffusion coefficients for the lithium ion in the TFSA-based ionic liquids have been reported by means of ^{7}Li NMR, applying the pulsed gradient spin echo (PGSE) technique.[9−13] Moreover, more recently, direct measurements of ionic mobility of several ionic liquids using the electric field applying the PGSE NMR was performed.[14] In addition, the electrode kinetics of the Li/Li^+ couple, such as diffusion coefficients and rate constants in a wide range of ionic liquids, was also reported.[15]

To further understanding lithium ion transport and diffusion behavior in the TFSA-based ionic liquids at a molecular level, the knowledge of the solvation structure of the lithium ion in the ionic liquids is necessary. Several studies that utilized Raman/IR spectroscopy,[16−19,24−26] molecular dynamics simulations,[21,22] and ab initio calculations[22,23] have been published on this subject. Since Lassègues et al. reported (using Raman spectroscopy,[17]) for the first time that two $TFSA^-$'s exist as the first solvation sphere of the lithium ion in the TFSA-based ionic liquids, it has become well-accepted that a solvation number of the lithium ion in the TFSA based ionic liquids is 2 in the lithium ion mole fraction $x < 0.2$.[19,24,25] Furthermore, Lassègues et al. recently revealed that an apparent lithium ion solvation number in the TFSA-based ionic liquid decreases from 2 at a higher lithium ion mole fraction, which implies that oligomers may be formed where multiple lithium ions and $TFSA^-$ anions coexist.[26]

* Address correspondence to either author. (Y.U.) Phone: +81 92 642 2582. Fax: +81 92 642 2582. E-mail: yumeb@chem.kyushu-univ.jp. (S.T.) E-mail: s.tsuzuki@aist.go.jp.
† Kyushu University.
‡ Saga University.
§ National Institute of Advanced Industrial Science and Technology.
⊥ Central Research Institute of Electric Power Industry.

10.1021/jp100898h
Published on Web 04/28/2010

Not only the lithium ion solvation structure but also freedom of torsional motions of the flexible $TFSA^-$ affects their transport and diffusive properties. First, on the basis of ab initio calculations,[27] Johansson et al. have found conformational isomerism of a $TFSA^-$ anion in gas phase. Since then, it has been experimentally studied.[28−31] The trans isomer, in which two $-CF_3$ groups are located at the trans positions against the S−N−S plane, is a global minimum in neat ionic liquids, whereas the cis one also coexists in equilibrium with a slightly higher energy of 2−3 kJ mol^{-1}. Interestingly, when the lithium salt is added, the isomerization equilibrium of $TFSA^-$ shifts toward the cis side, and in contrast, the cis isomer is preferred to the trans one in the lithium ion first solvation sphere.[24−26] To obtain further insight into this stabilization of the cis $TFSA^-$ nearest the lithium ion, it is indispensable to evaluate the thermodynamic quantities, such as Gibbs free energy, $\Delta_{iso}G^0$; enthalpy, $\Delta_{iso}H^0$; and entropy, $\Delta_{iso}S^0$, quantitatively for the conformational isomerism of $TFSA^-$. However, these quantities have not yet been evaluated, even in the neat ionic liquids.

In this paper, thermodynamic quantities of the conformational isomerism of $TFSA^-$ in neat $[C_4mIm][TFSA]$ ($[C_4mIm]$:1-butyl-3-methylimidazolium) ionic liquid and that in the first solvation sphere of the lithium ion in the ionic liquid were evaluated for the first time by means of Raman spectroscopy. Experimentally, in the $[C_4mIm][TFSA]$ containing also LiTFSA, it is indicated that the cis $TFSA^-$ was more stabilized than the trans at the nearest neighbor of the lithium ion with relatively large and negative enthalpy, though the reverse is the case in the neat $[C_4mIm][TFSA]$. To yield further insight into this enthalpic stabilization of the cis isomer, MP2 level ab initio calculations were also carried out. From the experimental and theoretical evidence, it is clearly indicated that intermolecular electrostatic interactions between the lithium ion solvated cluster of $[Li(cis\text{-}TFSA)_2]^-$ and the surrounding imidazolium cations play a key role in the cis $TFSA^-$ stabilization in the first solvation sphere of the lithium ion.

Experimental Section

Materials. Sample $[C_4mIm][TFSA]$ ionic liquid was synthesized by an ordinary method.[32−34] The water content was checked by a Karl Fischer titration to be less than 20 ppm, and the halide ion presence was checked by a $AgNO_3$ test to be negligible. LiTFSA salt (Morita Chemical Industries Co. Ltd.) was dried in vacuo at 425 K for one day and used without further purification. All materials were treated and stored in a high-performance glovebox equipped with moisture and oxygen sensors (MIWA MFG Co. Ltd.), in which the water and oxygen contents were kept less than 1 ppm. Lithium ion mole fractions of the sample liquids, x_{Li}, were 0.000 (neat ionic liquids), 0.053, 0.106, and 0.171.

Raman Spectra Measurements and Data Analyses. Details of the Raman spectra measurements were similar to our previous Raman studies.[24,30] Raman measurements at varying semperatures were carried out at 273, 294, 311, 330, 347, and 367 K with a hermetically sealed quartz cell whose temperature fluctuation was kept within ±0.3 K at a given temperature during the measurement. The sample room was filled with dry nitrogen gas to avoid condensation of moisture on the surface of the Raman cell at low temperature. Here, we briefly describe the Raman spectra correction employed in this study. Raw Raman spectra were corrected in terms of solution densities, which had been measured in advance at the respective lithium salt mole fraction and temperature corresponding to those in Raman measurements, and were normalized on the basis of an adequate Raman band arising from the $[C_4mIm]$ cation.[35−40] By using the thus corrected Raman intensity, $I(\nu)$, Raman spectra are represented as a form of the reduced Raman intensity, $R(\nu)$, given as follows,

$$R(\nu) \equiv I(\nu)(\nu_0 - \nu)^{-4}\nu[1 - \exp(-hc\nu/kT)] \qquad (1)$$

where ν_0 and ν cm^{-1} represent the frequencies of the irradiated laser light and Raman shift, respectively, and the others have the usual meanings.[41] The obtained $R(\nu)$ spectra were deconvoluted into single components of pseudo-Voigt functions by nonlinear least-squares analyses.

With Raman spectra of ionic liquids dissolving a metal salt, one may frequently divide solvent molecules (ions) into two approximate kinds: Those bound and those not bound to the metal ion. (Hereafter, we call the former and the latter ions *bound* and *free*, respectively.) Within such an approximation, the solvation number of the metal ion can be evaluated. To yield the solvation number of the lithium ion in the ionic liquid, the following procedure in our previous study[19,24,54] was adopted. The integral intensity, I_f, of the deconvoluted Raman band of the free $TFSA^-$ in the bulk ionic liquid is given as $I_f = J_f c_f$, where J_f and c_f stand for the molar Raman scattering coefficient and the concentration of the free $TFSA^-$ in the bulk, respectively. The c_f is given as $c_f = c_T - c_b = c_T - nc_{Li}$, where c_T and c_b denote the concentrations of total and bound $TFSA^-$ (solvated to the lithium ion), respectively, and c_{Li} and n denote the concentration and the solvation number of the lithium ion, respectively. By inserting the equation into $I_f = J_f c_f$, the following relationship was obtained: $I_f/c_{Li} = J_f(c_T/c_{Li} - n)$. If the solvation number of the lithium ion in the ionic liquid is kept unchanged under the examined experimental conditions, the plots of I_f/c_{Li} against R should give a straight line; thus, the value of n is obtained as $n = -\beta/\alpha$ from a slope $\alpha = J_f$ and an intercept $\beta = -J_f n$.

Quantum Calculations. The procedures for the B3LYP/6-311+G(d,p) level DFT calculations of the lithium ion solvated clusters were similar to those described in our previous study.[24] The formation energies (E_{form}) for the $[Li(trans\text{-}TFSA)_2]^-$ and $[Li(cis\text{-}TFSA)_2]^-$ clusters from isolated ions were calculated for evaluating the isomerization energy between the two clusters. The formation energies for the $[C_2mIm][Li(trans\text{-}TFSA)_2]$ and $[C_2mIm][Li(cis\text{-}TFSA)_2]$ clusters were also calculated for evaluating the effects of the $[C_2mIm]^+$ cation on the isomerization energy of the $TFSA^-$ anion. The E_{form} was given as the sum of the interaction energy (E_{int}) and the deformation energy (E_{def}) ($E_{form} = E_{int} + E_{def}$). The geometries of the clusters were optimized at the HF/6-311G(d,p) level. The E_{int} was calculated at the MP2/6-311G(d,p) level. The basis set superposition error was corrected by the counterpoise method.[42,43] The E_{def} is the sum of increases of the energies of ions by the deformations associated with the complex formation. The E_{def} was calculated at the MP2/6-311G(d,p)//HF/6-311G(d,p) level. All ab initio calculations were performed by using the Gaussian 03 program suite.[44]

Results and Discussion

Temperature Dependence of Raman Spectra and Li^+ Ion Solvation Structure. Figure 1 a, b shows the temperature dependence of the $R(\nu)$ spectra in the frequency range of 370−460 cm^{-1} for neat $[C_4mIm][TFSA]$ and that containing LiTFSA of $x_{Li} = 0.171$, respectively. This range of Raman spectra is suitable to discuss the $TFSA^-$ anion conformational

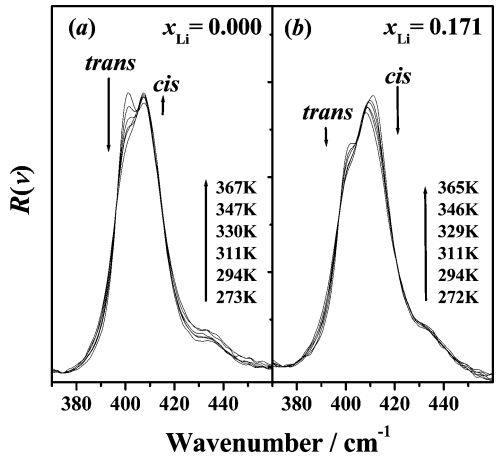

Figure 1. Temperature dependence of Raman spectra in the frequency range of 370−460 cm^{-1} as a form of the reduced Raman spectra $R(\nu)$ for (a) neat and (b) LiTFSA containing $x_{Li} = 0.171$ [C_4mIm][TSFA]. Temperatures are shown in the figures.

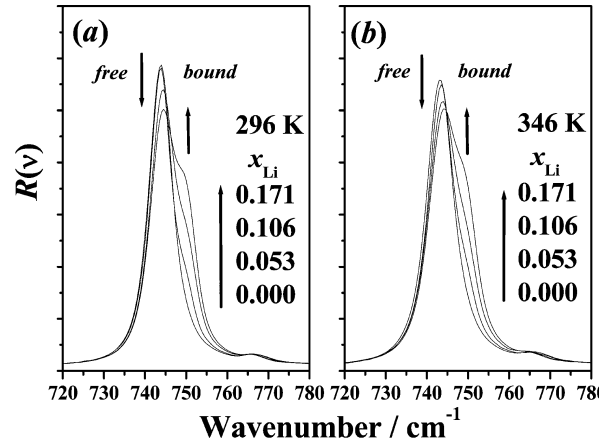

Figure 2. Lithium salt concentration dependences of the Raman spectra in the frequency range of 720−780 cm^{-1} for [C_4mIm][TFSA] ionic liquids containing LiTFSA salt at T = (a) 296 and (b) 346 K. The lithium salt mole fractions are shown in the respective panel.

isomerism[24,30] because the overlap with Raman bands from the $[C_4mIm]^+$ is not so serious, as shown in Supporting Information Figure S1.[35−40] Raman bands of 400 and 409 cm^{-1} are ascribable to the trans and cis isomers, respectively.[24−30] With regard to the neat ionic liquid, when the temperature increased, the Raman band of 400 cm^{-1} decreased, whereas that of 409 cm^{-1} slightly increased, indicating that the trans isomer is enthalpically stable relative to the cis isomer, as previously reported.[24−30] On the other hand, although lithium salt was dissolved, no new Raman bands appeared at the frequency range at the lithium salt concentrations and temperatures examined here, as shown in Figure 1b, which indicates that $TFSA^-$ yields similar Raman bands at this frequency range, even binding to the lithium ion. However, the relative intensity of the cis conformer was evidently larger than that of the trans at 272 K. Furthermore, although the peak height of both Raman bands decreased with increasing temperature, the intensity decrease of the band of 409 cm^{-1} was slightly larger than that of the other. These facts indicate that when $TFSA^-$ binds to the lithium ion in the ionic liquid, the cis isomer is more stabilized, relative to the trans, and the equilibrium population may shift toward the cis side, although qualitatively, this implies that the isomerization free energy and enthalpy for the solvated $TFSA^-$ should be relatively large.

As previously reported,[20,25−27] the lithium ion in TFSA-based ionic liquids is solvated by two $TFSA^-$ anions below $x_{Li} = 0.2$ at ambient temperature so that in the sample of $x_{Li} = 0.171$, about 34 mol % $TFSA^-$ must be solvated and the rest remain in the bulk. Therefore, it should be noted that the temperature dependence of the Raman spectra shown in Figure 1b is apparent. In other words, we can only observe the superposed Raman bands from the $TFSA^-$ anions in both the bulk and the first solvation sphere of the lithium ion in an ionic liquid.

Here, further attention should be paid to the following equilibrium:

$$[Li(TFSA)_2]^- \leftrightarrow [Li(TFSA)] + TFSA^- \qquad (2)$$

and in TFSA-based ionic liquids, may depend on the temperature, as previously pointed out by Lassègues et al.[17] In addition, the possibility of changes in the solvation manner of monodentate $TFSA^-$ must be accounted for, as pointed out in previous MD simulations.[20,21] Therefore, if the solvation structural changes in number and manner occur at higher temperatures, such structural changes may also contribute to the apparent thermodynamic quantities for the $TFSA^-$ isomerism.

For further quantitative discussion on the $TFSA^-$ isomerism, one must evaluate the solvation number of the lithium ion in the TFSA-based ionic liquid at ambient and higher temperatures, 296 and 346 K. Figure 2 represents lithium ion concentration dependences of Raman spectra at the frequency range of 720−780 cm^{-1} at 296 and 346 K, respectively. The intense Raman band at 744 cm^{-1} is ascribable to the CF_3 bending vibration $\delta_s(CF_3)$ coupled with the S−N stretching one $\nu_s(S-N-S)$ of the bulk $TFSA^-$.[43−45] At 296 K in Figure 2a, the peak intensity decreased with an increase in the lithium salt concentration. A new band at 750 cm^{-1}, which can be attributed to the same vibration mode, appeared upon the addition of LiTFSA salt, and its intensity increased with a pseudo-isosbestic point with the increase in the lithium concentration. Thus, this new band of 750 cm^{-1} can be ascribable to the $TFSA^-$ solvated to the lithium ion, as previously reported.[19,24−26] As mentioned in the Experimental section, we refer to the 744 and 750 cm^{-1} bands at 246 K and each corresponding band at higher temperature as free and bound, respectively.

At the higher temperature of 346 K, a similar variation with an increase in the lithium salt concentration was also found, as shown in Figure 2b, although the peak positions and band widths were shifted and broadened slightly as compared with those at 296 K. Although the peak positions of the Raman bands shifted toward the lower frequency side relative to those at ambient temperature, the difference of the peak positions, $\Delta\nu$, between the free and the bound $TFSA^-$ remained almost constant with increasing temperature, which indicates that no significant structural changes occur with respect to solvation number and manner for the lithium ion in the examined temperature range.

According to the procedures described in the Experimental section, the number of the $TFSA^-$ solvated to the lithium ion in the ionic liquid can be evaluated from the I_f/c_{Li} vs c_T/c_{Li} plots and was found to be 1.85(2) and 1.84(1) at 296 and 346 K, respectively, as shown in Figure 3. The agreement is very good between the two temperatures, and the value at the ambient temperature is consistent with those reported in previous studies.[19,24−26] It is clearly demonstrated that the solvation number is almost the same at the different temperatures. If the experimental errors were taken into consideration, the number of solvated $TFSA^-$ is about 2, and thus, the lithium ion should

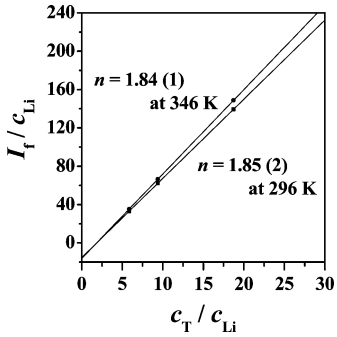

Figure 3. Determination of lithium ion solvation number from the I_f/c_{Li} vs c_T/c_{Li} plots of the lithium concentration dependence of Raman spectra in the frequency range of 720−780 cm^{-1} for $[C_4mIm][TFSA]$ ionic liquids containing LiTFSA salt measured at $T = 296$ and 346 K.

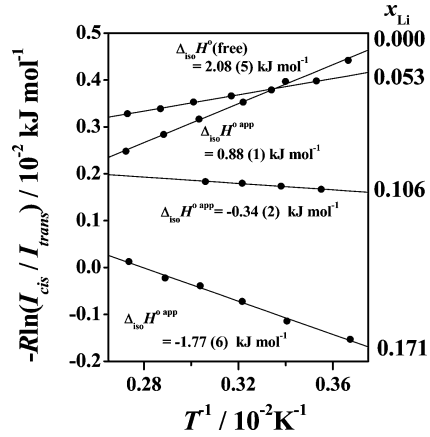

Figure 4. van't Hoff plots for determination of apparent thermodynamics quantities for the TFSA isomerism in $[C_4mIm][TFSA]$ ionic liquids containing LiTFSA salt $x_{Li} = 0.000$, 0.053, 0.106, and 0.171 in the temperature range of 273−350 K.

adopt a four-coordinated structure at both 296 and 346 K, since the TSFA anion is bidentate. It should be emphasized that the solvation number of the lithium ion was unchanged in the temperature range examined between 273 and 367 K.

The Raman experimental facts suggest that the intrinsic thermodynamic quantities for the conformational isomerism of $TFSA^-$ not only in the bulk but also in the first solvation sphere of the lithium ions can be evaluated via apparent thermodynamic quantities as a function of the lithium ion mole fraction. Overall errors in solvation numbers are, at most, 10% by our Raman measurements and analyses. It is possible to afford the information on the desolvation of lithium ions ($TFSA^-$ solvation number decease) with good accuracy (few percent in error). Supposing that the equilibrium represented in eq 2 was established, we can evaluate the corresponding enthalpy change to be 100−150 kJ mol^{-1}. The enthalpy change in decrease of the solvation number given in eq 2 should be large and positive: $\Delta H^0 > 0$, arising from the Li^+−O bond(s) disruption (O belonging to $TFSA^-$). Desolvated $TFSA^-$ from the first solvation sphere should be liberated into the bulk ionic liquid, where the $TFSA^-$ interacts with the ionic liquid cation. According to gas phase quantum calculations,[23,48] the formation energy E_{form} between a typical ionic liquid cation and $TFSA^-$ is much smaller (less negative) than that for the Li^+−$TFSA^-$. For instance, the values of E_{form} are −336.8 and −574.0 kJ mol^{-1} for C_2mIm^+−$TFSA^-$ and Li^+−$TFSA^-$, respectively. The difference of 237.2 kJ mol^{-1} is the same order of magnitude as the above estimation and predominates in ΔH^0 for the $TFSA^-$ solvation number decrease, although the solvation energy of the respective species may actually affect the ΔH^0 in ionic liquid solutions. It is supposed that the corresponding entropy change must also be positive, $\Delta S^0 > 0$, because the liberated $TFSA^-$ acquires larger entropy relative to the $TFSA^-$ tightly bound to the lithium ion of the small ionic radii. The freedom of motion of the $TFSA^-$ in bulk ionic liquids is also small due to the strong liquid structure of ionic liquids. Thus, the Gibbs free energy change for the decrease in the lithium ion solvation number must be positive: $\Delta G^0 = \Delta H^0 - T\Delta S^0 > 0$. Therefore, it is reasonable that the solvation number of the lithium ion in the TFSA-based ionic liquids is kept constant in the temperature range examined here.

Thermodynamic Quantities for TFSA Isomerism. As the next step, we attempted to determine the apparent thermodynamic quantities $\Delta_{iso}G^{0app}$, $\Delta_{iso}H^{0app}$, and $T\Delta_{iso}S^{0app}$ from the trans to cis isomers as a function of x_{Li}. For this purpose, van't Hoff plots at the individual x_{Li} are useful. Here, the apparent equilibrium constant, K_{iso}, for the $TFSA^-$ conformational isomerism from the trans to cis forms as a function of x_{Li} is defined as $K_{iso} = c_{cis}/c_{trans}$. The $\Delta_{iso}G^{0app}$ can be written as $\Delta_{iso}G^{0app} = -RT \ln K_{iso} = -RT \ln(c_{cis}/c_{trans})$. Here, R stands for a gas constant. If we take into consideration that the Raman band intensity I can be represented as $I = Jc$ using the Raman scattering coefficient J and a concentration of the scattering species c, eq 3 can be derived,

$$-R \ln(I_{cis}/I_{trans}) = \Delta_{iso}H^{0app}/T - \Delta_{iso}S^{0app} - R(J_{cis}/J_{trans}) \quad (3)$$

where J_{cis} and J_{trans} denote Raman scattering coefficients for the cis and the trans isomers of $TFSA^-$, respectively. Since the Raman spectra at the frequency range of 370−460 cm^{-1} in Figure 1 are suitable for the quantitative analyses of the conformational isomerism of $TFSA^-$,[30,31] the integral intensities of Raman bands I_{cis} and I_{trans} of 400 and 409 cm^{-1} were estimated with nonlinear least-squares analyses using pseudo-Voigt functions represented as a linear combination of Gauss and Lorentz functions (Figure S1 of the Supporting Information).

As shown in Figure 1, when adding and increasing the concentration of lithium ion, no significant variation of the Raman bands was observed in the peak position and bandwidth, and no new Raman band appeared up to $x_{Li} = 0.171$ (most concentrated sample). This seems to be inconsistent with theoretical Raman bands for $[Li(cis\text{-}TFSA)_2]^-$, $[Li(cis\text{-}TFSA)(trans\text{-}TFSA)]^-$ and $[Li(trans\text{-}TFSA)_2]^-$ at the B3LYP/6-311+G(d,p) level,[25] which is also shown in Supporting Information Figure S1. However, we have often seen that systematic and much larger deviations are found in the low frequency region in the plots of predicted $TFSA^-$ Raman bands vs the observed ones, which suggests that theoretical prediction of Raman bands of such a low frequency region are less reliable. Therefore, we assumed that the spectral change in the $TFSA^-$ Raman bands in this frequency range is practically negligible upon binding to the lithium ion. In fact, the peak parameters refined by nonlinear least-squares fitting hardly depend on x_{Li}. Thus, I_{trans} and I_{cis} were simply evaluated as integral intensities from the Raman bands of 400 and 409 cm^{-1}, respectively.

In the van't Hoff plots in Figure 4, the all plots of $-R \ln(I_{cis}/I_{trans})$ versus $1/T$ showed good, straight lines for the four x_{Li}'s, and clearly, the slopes strongly depend on x_{Li}; that is, the slopes changed from positive for $x_{Li} = 0.000$ (neat ionic liquid) to negative for the lithium salt containing one, and the values

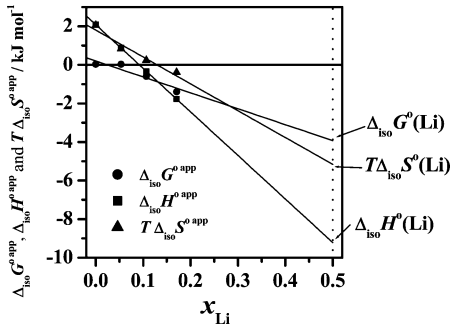

Figure 5. Apparent thermodynamic quantities for the conformational isomerism of TFSA from the trans to the cis isomer as a function of x_{Li} in [C_4mIm][TFSA] ionic liquids containing LiTFSA. $\Delta_{iso}G^{0app}$ corresponds to that at $T = 298$ K, and $\Delta_{iso}X^0$ (Li) (X: G, H, and S) were determined at $x_{Li} = 0.5$, assuming $n = 2$.

decreased according to the lithium concentrations. The results indicate that the slopes ($= \Delta_{iso}H^{0app}$) can be evaluated as the function of the x_{Li} with sufficient accuracy. As shown in eq 3, the $\Delta_{iso}S^{0app}$ can be estimated from the intercept of the van't Hoff plots if the ratio J_{cis}/J_{trans} is known. The value should be estimated by experiments or theoretical calculations because J_{cis} and J_{trans} are generally not the same, even if they can be ascribed to the same vibration mode.

From the relationship of $I_{cis} = J_{cis}c_T - (J_{cis}/J_{trans})I_{trans}$, the J_{cis}/J_{trans} can be experimentally determined from the slope of the plots of the I_{cis} against the I_{trans}. Since no significant variations of Raman spectra or peak function parameters depending on x_{Li} ware observed, the plots fall on a single, straight line to yield the value of 0.64 as the J_{cis}/J_{trans}. Theoretically estimated values of the J_{cis}/J_{trans} were 0.68, 0.69, 0.68, and 0.56 at the HF/6-31G(d), B3LYP/6-31G(d), 6-311+G(d) and 6-311+G(3df) levels, respectively, which are in good agreement with the experimental values.

The $\Delta_{iso}S^{0app}$ values were obtained from the intercepts of the van't Hoff plots in Figure 4. The values of the $\Delta_{iso}H^{0app}$, $\Delta_{iso}S^{0app}$, and $\Delta_{iso}G^{0app}$ ($= \Delta_{iso}H^{0app} - T\Delta_{iso}S^{0app}$) at 298 K were obtained for each x_{Li}, and the $\Delta_{iso}G^{0app}$, ΔH^{0app}, and $T\Delta_{iso}S^{0app}$ were plotted against the x_{Li} in Figure 5. All the plots fell on straight lines, suggesting that the apparent thermodynamic quantities $\Delta_{iso}X^{0app}$ (X: G, H, and S) can be represented as linear functions of the x_{Li}. As evidently shown in Figure 2, the $TFSA^-$ in lithium salt solutions can be described with a two-state model; that is, one exists in the first solvation sphere of the lithium ion, and the other is in the bulk. In this case, the following relationship holds.

$$\Delta_{iso}X^{0app} = nx_{Li}\,\Delta_{iso}X^0(\mathrm{Li}) + (1 - nx_{Li})\,\Delta_{iso}X^0(\mathrm{bulk}) \quad (4)$$

where $\Delta_{iso}X^0$(Li) and $\Delta_{iso}X^0$(bulk) represent the intrinsic thermodynamic quantities for the $TFSA^-$ in the first solvation sphere of the lithium ion and in the bulk, respectively. It should be noted that the solvation number $n = 2$ is constant under the examined conditions. Therefore, the least-squares analyses yield $\Delta_{iso}X^0$(bulk) and $\Delta_{iso}X^0$(Li) at $x_{Li} = 0$ and 0.5, respectively, as shown with the solid lines in Figure 5. The experimental intrinsic thermodynamic quantities for the $TFSA^-$ conformational isomerism both in the bulk and in the first solvation sphere of the lithium ion are listed in Table 1. The values of $\Delta_{iso}G^0$(bulk), $\Delta_{iso}H^0$(bulk), and $T\Delta_{iso}S^0$(bulk) evaluated at 298 K are 0.2(2), 2.08(1), and 1.8(2) kJ mol^{-1}, respectively. The value of $\Delta_{iso}H^0$(bulk) obtained in this study agrees well within the experimental errors with those previously reported from both experimental measurements[30,31] and theoretical calculations.[27,45−52] The trans isomer of $TFSA^-$ is enthalpically stable relative to the cis in the neat [C_4mIm][TFSA]; however, the latter is entropically more favorable than the former, and as the result, the Gibbs free energies of both isomers are almost similar.

When $TFSA^-$ anions bound to a lithium ion in the ionic liquid, dramatic changes in the situations were observed. The $\Delta_{iso}H^0$(bulk) of 2.08 kJ mol^{-1} becomes the $\Delta_{iso}H^0$(Li) of −9.2(1) kJ mol^{-1}, and the $T\Delta_{iso}S^0$(Li) value of −5(1) kJ mol^{-1} cannot compensate for the enthalpy. Thus, the $\Delta_{iso}G^0$(Li) of −4(1) kJ mol^{-1} remains large and negative, which indicates that the cis isomer of the $TFSA^-$ bound to the lithium ion is preferred relative to the trans due to the enthalpic stabilization. The large and negative enthalpy suggests that the stabilization of the $TFSA^-$ cis isomer in the first solvation sphere of the lithium ion can be attributed to specific interactions between the cis and the central lithium ion.

In our previous study,[25] we deduced that the specific interaction originates from a relatively large charge−dipole interaction between the lithium ion and the $TFSA^-$ cis isomer. In fact, the values of the dipole moment estimated with quantum calculations were 4.654, 5.420, 4.382, and 4.404 D for the cis isomer and 0.346, 0.299, 0.153, and 0.301 D for the trans at the HF/6-31G(d), B3LYP/6-31G(d), B3LYP/6-311+G(d), and B3LYP/6-311+G(3df) levels, respectively.[30] However, according to our previous DFT calculations at the B3LYP/6-311+G(d,p) level, the energies for [Li(*cis*-TFSA)$_2$]$^-$ and [Li(*cis*-TFSA)(*trans*-TFSA)]$^-$ relative to that for [Li(*trans*-TFSA)$_2$]$^-$ were calculated to be 1.0 and 0.0 kJ mol^{-1}, respectively, although the binding energies estimated as $\Delta E = E$ (lithium ion solvated cluster) $- E(\mathrm{Li}^+) - 2E$ (the corresponding $TFSA^-$ isomers) are −792.5, −791.2, and −788.9 kJ mol^{-1} for [Li(*cis*-TFSA)$_2$]$^-$, [Li(*cis*-TFSA)(*trans*-TFSA)]$^-$ and [Li(*trans*-TFSA)$_2$]$^-$, respectively.[25] Here, we revisit our theoretical approaches with additional new calculations based on the MP2 level as described in the following section.

Quantum Calculations. Isomerization energy, $\Delta_{iso}E^0$, and the corresponding thermodynamic quantities $\Delta_{iso}H^0$, $T\Delta_{iso}S^0$, and $\Delta_{iso}G^0$ for the $TFSA^-$ anions in solvated clusters around one lithium ion from [Li(*trans*-TFSA)$_2$]$^-$ to [Li(*cis*-TFSA)(*trans*-TFSA)]$^-$ (step 0 → 1) and those from [Li(*cis*-TFSA)(*trans*-TFSA)]$^-$ to [Li(*cis*-TFSA)$_2$]$^-$ (step 1 → 2) were calculated at the B3LYP/6-311G+(d,p) level. With the respective isomerism step, the values of $\Delta_{iso}E^0$ are 0.0 and 1.0 kJ mol^{-1} for steps 0 → 1 and 1 → 2, respectively, which are close to zero. On the other hand, the $\Delta_{iso}H^0$ of 5.9 and 6.0 kJ mol^{-1} for steps 0 → 1 and 1 → 2 are large and positive. $\Delta_{iso}H^0$ of almost the same values at the same level of theory has been reported by Lassègues et al.[26] It should be noted that the values are inconsistent with the Raman experimental facts. The $\Delta_{iso}G^0$ evaluated to be 7.2 and 4.1 kJ mol^{-1} for steps 0 → 1 and 1 → 2, respectively, also disagree with the Raman experimental values. The discrepancy in $\Delta_{iso}H^0$ and $\Delta_{iso}G^0$ must be due to large values of the zero point energy. We thus calculated $\Delta_{iso}E^0$ from the E_{form} of [Li(*trans*-TFSA)$_2$]$^-$ and [Li(*cis*-TFSA)$_2$]$^-$ at the MP2/6-311G(d,p) level. The calculated $\Delta_{iso}E^0$ value from [Li(*trans*-TFSA)$_2$]$^-$ to [Li(*cis*-TFSA)$_2$]$^-$ of 13.8 kJ mol^{-1} was large. A large discrepancy was also seen for the experimental $\Delta_{iso}H^0$(Li) of −9.2 kJmol^{-1}. Therefore, we should revise our previous speculation for the stabilization with the charge−dipole interaction model between the lithium ion and the cis isomer of $TFSA^-$ in ionic liquids.

TABLE 1: Thermodynamic Quantities for the Isomerism of $TFSA^-$ from the Trans to the Cis Isomer in Bulk and That in the First Solvation Sphere of the Lithium Ion in [C_4mIm][TFSA] and Related Ionic Liquids Evaluated by Raman Spectroscopy, MD Simulations and MO Calculations at 298 K[a]

	bulk				Li^+ first solvation sphere					
			MO				MO			
							DFT[b]		ab initio[c]	
	Raman	MD	DFT[b]	ab initio[c]	Raman	MD	0 → 1[d]	1 → 2[e]	isolated[f]	[C_2mIm] [g]
$\Delta_{iso}G^0$	0.2 (2)	0.6 (1)	2.1		−4 (1)	−1.1 (4)	7.2	4.1		
$\Delta_{iso}H^0$	2.08 (1)		3.1		−9.2		5.9	6.0		
$T\Delta_{iso}S^0$	1.8 (2)		1.0		−5 (5)		−1.3	1.9		
$\Delta_{iso}E$				5.4			0.0	1.0	13.8	−8.8

[a] All thermodynamic quantities are given in kJ mol^{-1}. [b] B3LYP/6-311+G(d,p). Thermodynamic quantities were not scaled. [c] MP2/6-311G(d,p). [d] From [Li(*trans*-TFSA)$_2$]$^-$ to [Li(*cis*-TFSA)(*trans*-TFSA)]$^-$. [e] From [Li(*cis*-TFSA)(*trans*-TFSA)]$^-$ to [Li(*cis*-TFSA)$_2$]$^-$. [f] Without [C_2mIm]. [g] With [C_2mIm].

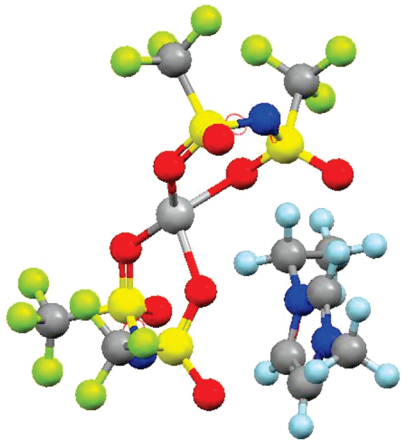

Figure 6. Optimized geometry for the [C_2mIm][Li(*cis*-TFSA)$_2$] of the lowest energy in the gas phase at the MP2/6-311G(d,p) levels of theory.

On the other hand, according to our MD simulations for similar systems of [Li$x_{Li}C_2mIm_{(1-x_{Li})}$TFSA] ($x_{Li}$ = 0, 0.15, and 0.32), the cis isomer evidently increased with increasing lithium ion concentration.[53] In the simulations, the estimated values of $\Delta_{iso}G^0$ for the conformational isomerism of $TFSA^-$ from the trans to the cis isomers in the neat and in the first solvation sphere of a lithium ion were 0.6 and −1.1 kJ mol^{-1}, respectively, which qualitatively agrees with the Raman experiments. Thus, the MD simulations indicate that the specific stabilization of the $TFSA^-$ cis isomer in the first solvation shell of the lithium is ascribable to the intermolecular interactions between the lithium ion solvated cluster and the surrounding imidazolium cation.

To clarify the effect of the C_2mIm cation, $\Delta_{iso}E^0$ was calculated from the E_{form} of [C_2mIm][Li(*trans*-TFSA)$_2$] and [C_2mIm][Li(*cis*-TFSA)$_2$] at the MP2/6-311G(d,p) level. The E_{form} for several configurations was calculated (Supporting Information Figure S3), then the configuration of the lowest energy was found for [C_2mIm][Li(*cis*-TFSA)$_2$] (Figure 6). All configurations of [C_2mIm][Li(*trans*-TFSA)$_2$] were higher in energy relative to the lowest one. The value of the $\Delta_{iso}E^0$ was evaluated to be −8.8 kJ mol^{-1}, which is in good agreement with $\Delta_{iso}H^0$(Li) obtained by Raman experiments.

Two-body interaction energies in the [C_2mIm][Li(*cis*-TFSA)$_2$] and [C_2mIm][Li(*trans*-TFSA)$_2$] clusters (E_{Int}(X−Y), X, Y = Li^+, TFSA1$^-$, TFSA2$^-$, and C_2mim^+) were summarized in Table 2. The two $TFSA^-$ anions in each cluster are not equivalent, and therefore, they are called TFSA1$^-$ and TFSA2$^-$, as shown in Figure 7. Although the size of six types of two-body interaction energies in the clusters is significant (more than 200 kJ mol^{-1}), the difference between the same type of two-body interactions for the two clusters are small (less than 8 kJ mol^{-1}), except the E_{int}(TFSA1$^-$-C_2mim^+). The E_{int}(TFSA1$^-$−C_2mim^+) for the [C_2mIm][Li(*cis*-TFSA)$_2$] is −29.3 kJ mol^{-1} more negative than that for the [C_2mIm][Li(*trans*-TFSA)$_2$], which shows that the large attraction between the TFSA1$^-$ and C_2mim^+ is mainly responsible for the larger stability of the [C_2mIm][Li(*cis*-TFSA)$_2$] as compared with the [C_2mIm][Li(*trans*-TFSA)$_2$]. It should be noted that the E_{int}(TFSA1$^-$−C_2mIm^+) of −322.9 kJ mol^{-1} for [C_2mIm][Li(*cis*-TFSA)$_2$] is almost similar to the E_{int} of −329.7 kJ mol^{-1} evaluated for the most stable isolated C_2mIm^+−$TFSA^-$ complex.[48] The many-body interaction energy ($E_{many\text{-}body}$) is the difference between the total interaction energy (E_{int}) and the sum of two-body interaction energies (ΣE_{int}(X−Y)) ($E_{many\text{-}body} = E_{int} - \Sigma E_{int}$(X−Y)). The $E_{many\text{-}body}$ values for the two clusters are nearly identical (the difference is less than 2 kJ mol^{-1}), which shows that the many-body interaction is not the cause of the stability of [C_2mIm][Li(*cis*-TFSA)$_2$].

We would like to discuss our finding from the viewpoint of metal ion stabilization mechanisms in solution. In general, the molecular structure of solvated molecules relative to a metal ion with a monodentate coordinative bonding manner varies little from that in bulk. However, in nonaqueous solvents having a flexible alkyl chain close to the donating atom, the alkyl chain flexibility induces the additional metal ion stabilization by solvating. Such stabilization was found in metal ion solutions of *N*,*N*-dimethylproionamide ($(CH_3)_2NCOC_2H_5$), where the solvent molecules change their conformation in the first solvation sphere to lower (to make more negative) the solvation enthalpy of the metal ion.[54−57] Similar stabilization of the lithium ion in dimethyl carbonate has been reported .[58−60] This additional stabilization in enthalpy is limited within the first solvation sphere of metal ions. In fact, such enthalpic stabilization can be reproduced in gas phase quantum calculations just for the metal ion solvated clusters of $[M(solvent)_n]^{z+}$.[57,59,60]

The E_{int} values calculated for the [Li(*trans*-TFSA)$_2$]$^-$ and [Li(*cis*-TFSA)$_2$]$^-$ clusters are not largely different, which shows that the interactions of the Li^+ cation with $TFSA^-$ anions do not stabilize the cis form of the $TFSA^-$ anion. On the other hand, the MP2 calculations indicate that the [C_2mIm][Li(*cis*-TFSA)$_2$] is substantially more stable than the [C_2mIm][Li(*trans*-TFSA)$_2$], which shows that the interactions of the [Li(*cis*-TFSA)$_2$]$^-$ with the C_2mIm^+ cation is the cause of the stability. Unique stabilization mechanisms of the [C_2mIm][Li(TFSA)$_2$] cluster by the interactions with the C_2mIm^+ are illustrated in

TABLE 2: Formation, Interaction and Deformation Energy E_{form}, E_{int} and E_{def}/kJ mol^{-1} for [C_2mIm][Li(*cis*-TFSA)$_2$] and [C_2mIm][Li(*trans*-TFSA)$_2$] in Gas Phase Calculated at the MP2/6-311G(d,p)/HF/6-311(d,p) Levels of Theory[a]

	[C_2mIm][Li(*cis*-TFSA)$_2$]	[C_2mIm][Li(*trans*-TFSA)$_2$]	Δ
E_{form}	−1053.8	−1045.0	−8.8
E_{int}	−1107.3	−1088.9	−18.4
E_{def}	53.4	43.9	9.6
E_{int}(Li^+−TFSA1$^-$)	−582.2	−586.2	3.9
E_{int}(Li^+−TFSA2$^-$)	−587.0	−583.1	−3.9
E_{int}(Li^+−C_2mIm^+)	262.3	257.1	5.2
E_{int}(TFSA1$^-$−TFSA2$^-$)	265.8	258.6	7.1
E_{int}(TFSA1$^-$−C_2mIm^+)	−322.9	−293.6	−29.3
E_{int}(TFSA2$^-$−C_2mIm^+)	−292.6	−289.3	−3.3
ΣE_{int} (X−Y)[a]	−1256.7	−1236.5	−20.2
$E_{many\text{-}body}$	149.5	147.6	1.8

[a] Pair interaction energy between two ions involving [C_2mIm][Li(*cis*-TFSA)$_2$] and [C_2mIm][Li(*trans*-TFSA)$_2$] E_{int}(X−Y)/kJ mol^{-1} (X, Y: Li^+, TFSA1$^-$, TFSA2$^-$, C_2mIm^+) at the same level of theory. [b] ΣE_{int}(X−Y) = E_{int}(Li^+−TFSA1$^-$) + E_{int}(Li^+−TFSA2$^-$) + E_{int}(Li^+−C_2mIm^+) + E_{int}(TFSA1$^-$−TFSA2$^-$)E_{int}(TFSA1$^-$−C_2mIm^+) + E_{int}(TFSA2$^-$−C_2mIm^+). [c] $E_{many\text{-}body}$ = E_{int} − ΣE_{int}(X−Y).

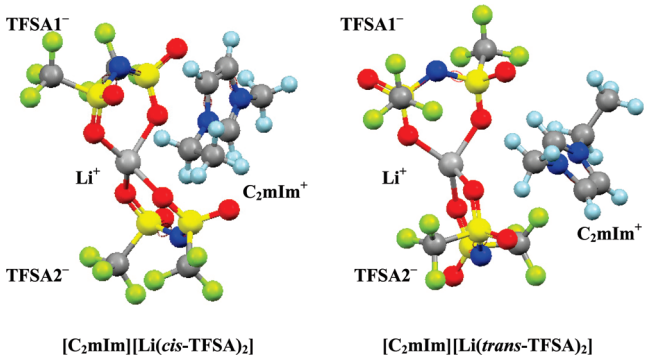

Figure 7. The respective most stable configuration for [C_2mIm][Li(*cis*-TFSA)$_2$] and [C_2mIm][Li(*trans*-TFSA)$_2$] and the definition of Li^+, TFSA1$^-$, TFSA2$^-$, and C_2mIm^+ for calculation of E_{int}(X−Y).

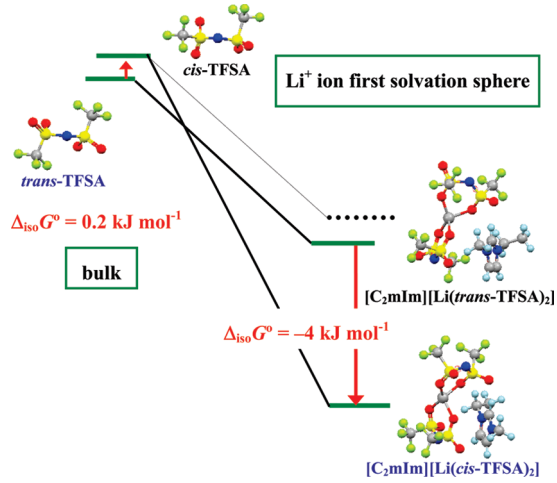

Figure 8. Schematic illustration of lithium ion stabilization solvated by two TFSAs in cis isomers, interacting with an imidazolium cation.

Figure 8. The *trans*-TFSA$^-$ is slightly stable relative to the *cis*-TFSA$^-$ in the neat ionic liquids. According to our quantum calculations for the [Li(TFSA)$_2$]$^-$ without the C_2mIm^+ cation, the donating ability or the Lewis basicity of TFSA$^-$ (or the acidity of a conjugated acid) are independent of the TFSA$^-$ conformations. It is supposed that the steric hindrance or electrostatic repulsion among the solvated TFSA$^-$ in the clusters of [Li(TFSA)$_2$]$^-$ are little different between trans and cis conformations. Consequently, thermodynamic quantities for the TFSA$^-$ conformational isomers should have similar values when it solvates to the lithium ion, as shown by the dashed line in Figure 8. However, the Raman spectra evidently revealed that the lithium ion solvated by the cis TFSA$^-$ isomers is more stabilized relative to the trans. As clearly suggested by ab initio calculations for the [C_2mIm][Li(TFSA)$_2$], the closest imidazolium cation(s) around [Li(TFSA)$_2$]$^-$ must be taken into account, and they play a key role. If we employ the hypothetical energy level shown as a dashed line in Figure 8 as the reference state, such an additional stabilization should contribute to the lithium ion solvation free energy in the TFSA-based ionic liquid. In other words, the central lithium ion is more stabilized in the solvation free energy via the TFSA$^-$ conformational isomerism with the aid of the surrounding cations than the second solvation sphere of the lithium ion.

Conclusions

Raman spectra of a flexible anion, TFSA$^-$ (CF_3−SO_2−N−SO_2−CF_3) in neat ionic liquids showed two CF_3 groups located at trans or cis positions against the S−N−S plane with each other, where the two CF_3−SO_2− conformations are not equivalent within a molecule, resulting in a nonsymmetric structure in a TFSA$^-$. In this study, Raman spectra of neat and lithium salt-containing ionic liquids [C_4mIm][TFSA] (the lithium ion mole fraction, x_{Li} = 0.053, 0.106, and 0.171) were measured with varying temperatures from 273 to 350 K. The number of solvated TFSA$^-$ to a lithium ion was 1.84 and 1.85 at 296 and 346 K, respectively, and was almost constant with increasing temperatures. In the neat ionic liquids, the trans isomer of TFSA$^-$ was shown to be slightly stable, and here, we quantitatively confirm the *cis*-TFSA$^-$ preferentially solvates to a lithium ion. The apparent thermodynamic quantities, such as $\Delta_{iso}G^{0app}$, $\Delta_{iso}H^{0app}$, and $\Delta_{iso}S^{0app}$, for the TFSA$^-$ conformational isomerism from the trans to cis isomers as a function of x_{Li}, were evaluated. The plots of the $\Delta_{iso}G^{0app}$, $\Delta_{iso}H^{0app}$, and $\Delta_{iso}S^{0app}$ determined at various x_{Li} fall on the respective straight lines; thus, intrinsic thermodynamic quantities, such as $\Delta_{iso}G^0$(bulk), $\Delta_{iso}H^0$(bulk), and $\Delta_{iso}S^0$(bulk) and $\Delta_{iso}G^0$(Li), $\Delta_{iso}H^0$(Li), and $\Delta_{iso}S^0$(Li) were determined with enough accuracy. $\Delta_{iso}G^0$(bulk) and $\Delta_{iso}H^0$(bulk) were 0.2 and 2.08 kJ mol^{-1} at 298 K, respectively, and agreed well with those previously reported. For the first time, $\Delta_{iso}G^0$(Li) and $\Delta_{iso}H^0$(Li) were experimentally determined to be −4 and −9.2 kJ mol^{-1} at 298 K, respectively. These intrinsic thermodynamic quantities suggest that the TFSA$^-$ cis isomers are enthalpically stabilized in the lithium ion first solvation sphere in the ionic liquids. The large and

negative value of $\Delta_{iso}H^0$(Li) suggests the isomerism operates to stabilize the solvated lithium ion system.

Gas phase quantum calculations were also carried out to yield more insight into this $TFSA^-$ conformational isomerism in the first solvation sphere of the lithium ion in the TFSA-based ionic liquids. We could not reproduce experimental $\Delta_{iso}H^0$(Li) by theoretical calculations for $[Li(cis\text{-}TFSA)_2]^-$, $[Li(cis\text{-}TFSA)(trans\text{-}TFSA)]^-$, and $[Li(trans\text{-}TFSA)_2]^-$. According to ab initio calculations at the MP2/6-311G(d,p) level for $[C_2mIm][Li(TFSA)_2]$, the most stable species was $[C_2mIm][Li(cis\text{-}TFSA)_2]$ rather than $[C_2mIm][Li(trans\text{-}TFSA)_2]$. Thus, theoretically predicted $\Delta_{iso}E^0$ from $[C_2mIm][Li(trans\text{-}TFSA)_2]$ to $[C_2mIm][Li(cis\text{-}TFSA)_2]$ were -8.8 kJ mol^{-1}, which reasonably agrees with the experimental $\Delta_{iso}H^0$(Li). Moreover, the specific stability of the *cis*-$TFSA^-$ isomers in the solvation sphere can be attributed to the electrostatic interaction between the solvated *cis*-$TFSA^-$ and the surrounding imidazolium cation.

The *cis*-$TFSA^-$ stabilization in the first solvation sphere of the lithium ion was found by Raman spectroscopic experiments and well-explained by the ab initio calculations due to specific intermolecular electrostatic interactions between the $TFSA^-$ in the lithium ion solvated cluster and the surrounding imidazolium cations.

Acknowledgment. This work has been financially supported by Grants-in-Aid for Scientific Research Nos. 19003963, 19350033, and 20350037, and for Scientific Research in Priority Area (Ionic Liquids) 20031024 from the MEXT.

Supporting Information Available: Additional information as noted in text. This material is available free of charge via the Internet at http://pubs.acs.org.

References and Notes

(1) *Electrochemical Aspects of Ionic Liquids*; Ohno, H., Ed.; John & Wiley Sons, Inc.: Hoboken, NJ, 2005.
(2) Tarascon, J.-M.; Armand, M. *Nature* **2001**, *414*, 359.
(3) Sakaebe, H.; Matsumoto, H. *Electrochem. Commun.* **2003**, *5*, 594.
(4) Garcia, B.; Lavallee, S.; Perron, G.; Michot, C.; Armand, M. *Electrochim. Acta* **2004**, *49*, 4583.
(5) Katayama, Y.; Yukumoto, M.; Miura, T. *Electrochem. Solid-State Lett.* **2003**, *6*, A96.
(6) Seki, S.; Kobayashi, Y.; Miyashiro, H.; Ohno, Y.; Mita, Y.; Usami, A.; Terada, N.; Watanabe, M. *Electrochem. Solid-State Lett.* **2005**, *8*, A577.
(7) Seki, S.; Kobayashi, Y.; Miyashiro, H.; Ohno, Y.; Usami, A.; Mita, Y.; Kihara, N.; Watanabe, M.; Terada, N. *J. Phys. Chem. B* **2006**, *110*, 10228.
(8) Seki, S.; Ohno, Y.; Kobayashi, Y.; Miyashiro, H.; Usami, A.; Mita, Y.; Tokuda, H.; Watanabe, M.; Hayamizu, K.; Tsuzuki, S.; Hattori, M.; Terada, N. *J. Electrochem. Soc.* **2007**, *154*, A173.
(9) Nicotera, I.; Oliviero, C.; Henderson, W. A.; Appetecchi, G. B.; Passerini, S. *J. Phys. Chem. B* **2005**, *109*, 22814.
(10) Saito, Y.; Umecky, T.; Niwa, J.; Sakai, T.; Maeda, S. *J. Phys. Chem. B* **2007**, *111*, 11794.
(11) Umecky, T.; Saito, Y.; Okumura, Y.; Maeda, S.; Sakai, T. *J. Phys. Chem. B* **2008**, *112*, 3357.
(12) Hayamizu, K; Tsuzuki, S; Seki, S.; Ohno, Y.; Miyashiro, H.; Kobayashi, Y. *J. Phys. Chem. B* **2008**, *112*, 1189.
(13) Frömling, T; Kunze, M.; Schönhoff, M.; Sundermeyer, J.; Roling, B. *J. Phys. Chem. B* **2008**, *112*, 12985.
(14) Umecky, T; Saito, Y; Matsumoto, H. *J. Phys. Chem. B* **2009**, *113*, 8466.
(15) Wibowo, R; Jones, S. E. W.; Compton, R. G. *J. Chem. Eng. Data*, **2009**, ASAP.
(16) Castriota, M.; Caruso, T.; Agostino, R. G.; Cazzanelli, E.; Henderson, W. A.; Passerini, S. *J. Phys. Chem. A* **2005**, *109*, 92–96.
(17) Lassègues, J.-C.; Grondin, J.; Talaga, D. *Phys. Chem. Chem. Phys.* **2006**, *8*, 5629.
(18) Hardwick, L. J.; Holzapfel, M.; Wokaun, A.; Novák, P. *J. Raman Spectrosc.* **2007**, *38*, 110.
(19) Shirai, A.; Fujii, K.; Seki, S.; Umebayashi, Y.; Ishiguro, S.; Ikeda, Y. *Anal. Sci.* **2008**, *24*, 1291.
(20) Borodin, O.; Smith, G. D.; Henderson, W. *J. Phys. Chem. B* **2006**, *110*, 16879.
(21) Monteiro, M. J.; Bazito, F. F. C.; Siqueira, L. J. A.; Ribeiro, M. C. C.; Torresi, R. M. *J. Phys. Chem. B* **2008**, *112*, 2102.
(22) Gejji, S. P.; Suresh, C. H.; Babu, K.; Gadre, S. R. *J. Phys. Chem. A* **1999**, *103*, 7474.
(23) Tsuzuki, S.; Hayamizu, K.; Seki, S.; Ohno, Y.; Kobayashi, Y.; Miyashiro, H. *J. Phys. Chem. B* **2008**, *112*, 9914.
(24) Umebayashi, Y.; Mitsugi, T.; Fukuda, S.; Fujimori, T.; Fujii, K.; Kanzaki, R.; Takeuchi, M.; Ishiguro, S. *J. Phys. Chem. B* **2007**, *111*, 13028.
(25) Duluard, S.; Grondin, J.; Bruneel, J.-L.; Pianet, I.; Grélard, A.; Campet, G.; Delville, M.-H.; Lassègues, J.-C. *J. Raman Spectrosc.* **2008**, *39*, 627.
(26) Lassègues, J.-C.; Grondin, J.; Aupetit, C.; Johansson, P. *J. Phys. Chem. A* **2009**, *113*, 305.
(27) Johansson, P.; Gejji, S. P.; Tegensfeldt, J.; Lindgren, J. *Electrochim. Acta* **1998**, *43*, 1375.
(28) Herstedt, M.; Smirnov, M.; Johansson, P.; Chami, M.; Grondin, J.; Servant, L.; Lassègues, J.-C. *J. Raman Spectrosc.* **2005**, *36*, 762.
(29) Herstedt, M.; Henderson, W. A.; Smirnov, M.; Ducasse, L.; Servant, L.; Talaga, D.; Lassègues, J.-C. *J. Mol. Struct.* **2006**, *783*, 145.
(30) Fujii, K.; Kanzaki, R.; Takamuku, T.; Fujimori, T.; Umebayashi, Y.; Ishiguro, S. *J. Phys. Chem. B* **2006**, *110*, 8179.
(31) Umebayashi, Y.; Mitsugi, T.; Fujii, K.; Seki, S.; Chiba, K.; Yamamoto, H.; Lopes, J. N. C.; Pádua, A. A. H.; Takeuchi, M.; Kanzaki, R.; Ishiguro, S. *J. Phys. Chem. B* **2009**, *113*, 4338.
(32) Nockemann, P.; Binnemans, K.; Driesen, K. *Chem. Phys. Lett.* **2005**, *415*, 131.
(33) Earle, M. J.; Gordon, C. M.; Plechkova, N. V.; Seddon, K. R.; Welton, T. *Anal. Chem.* **2007**, *79*, 758.
(34) Burrel, A. R.; Del Sasto, R. E.; Baker, S. N.; McCleskey, T. M.; Baker, G. A. *Green Chem.* **2007**, *9*, 449.
(35) Hayashi, S.; Ozawa, R.; Hamaguchi, H. *Chem. Lett.* **2003**, *32*, 498.
(36) Saha, S.; Hayashi, S.; Kobayashi, A.; Hamaguchi, H. *Chem. Lett.* **2003**, *32*, 740.
(37) Ozawa, R.; Hayashi, S.; Saha, S.; Kobayashi, A.; Hamaguchi, H. *Chem. Lett.* **2003**, *32*, 948.
(38) Berg, R. W.; Deetlefs, M.; Seddon, K. R.; Shim, I.; Thompson, J. M. *J. Phys. Chem. B* **2005**, *109*, 19018.
(39) Holomb, R.; Martinelli, A.; Albinsson, I.; Lassègues, J.-C.; Johansson, P.; Jacobsson, P. *J. Raman Spectrosc.* **2008**, *39*, 793.
(40) Endo, T.; Kato, T.; Tozaki, K.; Nishikawa, K. *J. Phys. Chem. B* **2010**, *114*, 407.
(41) Fujii, K.; Kumai, K.; Takamuku, T.; Umebayashi, Y.; Ishiguro, S. *J. Phys. Chem. A* **2006**, *110*, 1798.
(42) Boys, S. F.; Bernardi, F. *Mol. Phys.* **1970**, *19*, 553.
(43) Simon, S.; Duran, M.; Dannenberg, J. J. *J. Chem. Phys.* **1996**, *105*, 11024.
(44) Frisch, M.J. Trucks, G. W.; Schlegel, H. B.; Scuseria, G. E.; Robb, M. A.; Cheeseman, J. R.; Montgomery, J. A., Jr.; Vreven, T.; Kudin, K. N.; Burant, J. C.; Millam, J. M.; Iyengar, S. S.; Tomasi, J.; Barone, V.; Mennucci, B.; Cossi, M.; Scalmani, G.; Rega, N.; Petersson, G. A.; Nakatsuji, H.; Hada, M.; Ehara, M.; Toyota, K.; Fukuda, R.; Hasegawa, J.; Ishida, M.; Nakajima, T.; Honda, Y.; Kitao, O.; Nakai, H.; Klene, M.; Li, X.; Knox, J. E.; Hratchian, H. P.; Cross, J. B.; Bakken, V.; Adamo, C.; Jaramillo, J.; Gomperts, R.; Stratmann, R. E.; Yazyev, O.; Austin, A. J.; Cammi, R.; Pomelli, C.; Ochterski, J. W.; Ayala, P. Y.; Morokuma, K.; Voth, G. A.; Salvador, P.; Dannenberg, J. J.; Zakrzewski, V. G.; Dapprich, S.; Daniels, A. D.; Strain, M. C.; Farkas, O.; Malick, D. K.; Rabuck, A. D.; Raghavachari, K.; Foresman, J. B.; Ortiz, J. V.; Cui, Q.; Baboul, A. G.; Clifford, S.; Cioslowski, J.; Stefanov, B. B.; Liu, G.; Liashenko, A.; Piskorz, P.; Komaromi, I.; Martin, R. L.; Fox, D. J.; Keith, T.; Al-Laham, M. A.; Peng, C. Y.; Nanayakkara, A.; Challacombe, M.; Gill, P. M. W.; Johnson, B.; Chen, W.; Wong, M. W.; Gonzalez, C.; Pople, J. A. *Gaussian 03, revision C.02*; Gaussian, Inc.: Wallingford, CT, 2004.
(45) Rey, I.; Johansson, P.; Lindgren, J.; Lassègues, J. C.; Grondin, J.; Servant, L. *J. Phys. Chem. A* **1998**, *102*, 3249.
(46) Huang, W.; Frech, R.; Wheeler, R. A. *J. Phys. Chem.* **1994**, *98*, 100.
(47) Bakker, A.; Gejji, S.; Lindgren, J.; Hermansson, K.; Probst, M. M. *Polymer* **1995**, *36*, 4371.
(48) Tsuzuki, S.; Tokuda, H.; Hayamizu, K.; Watanabe, M. *J. Phys. Chem. B* **2005**, *109*, 16474.
(49) Lopes, J. N. C.; Pádua, A. A. H. *J. Phys. Chem. B* **2004**, *108*, 16893.
(50) Borodin, O.; Smith, G. D. *J. Phys. Chem. B* **2006**, *110*, 11481.
(51) Lopes, J. N. C.; Shimizu, K.; Pádua, A. A. H.; Umebayashi, Y.; Fukuda, S.; Fujii, K.; Ishiguro, S. *J. Phys. Chem. B* **2008**, *112*, 1465.
(52) Lopes, J. N. C.; Shimizu, K.; Pádua, A. A. H.; Umebayashi, Y.; Fukuda, S.; Fujii, K.; Ishiguro, S. *J. Phys. Chem. B* **2008**, *112*, 9449.
(53) Umebayashi, Y.; Yamaguchi, T.; Fukuda, S.; Mitsugi, T.; Takeuchi, M.; Fujii, K.; Ishiguro, S. *Anal. Sci.* **2008**, *24*, 1297.
(54) Umebayashi, Y.; Matsumoto, K.; Mune, Y.; Zhang, Y.; Ishiguro, S. *Phys. Chem. Chem. Phys.* **2003**, *5*, 2552.

(55) Zhang, Y.; Watanabe, N.; Miyawaki, Y.; Mune, Y.; Fujii, K.; Umebayashi, Y.; Ishiguro, S. *J. Solution Chem.* **2005**, *34*, 1429.

(56) Asada, M.; Mitsugi, T.; Fujii, K.; Kanzaki, R.; Umebayashi, Y.; Ishiguro, S. *J. Mol. Liq.* **2007**, *136*, 138.

(57) Umebayashi, Y.; Mroz, B.; Asada, M.; Fujii, K.; Matsumoto, K.; Mune, Y.; Probst, M.; Ishiguro, S. *J. Phys. Chem. A* **2005**, *109*, 4862.

(58) Soetens, J.-C.; Millot, C.; Maigret, B. *J. Phys. Chem. A* **1998**, *102*, 1055.

(59) Ishiguro, S.; Umebayashi, Y.; Fujii, K.; Kanzaki, R. *Pure Appl. Chem.* **2006**, *78*, 1595.

(60) Borodin, O.; Smith, G. D. *J. Phys. Chem. B* **2009**, *113*, 1763.

JP100898H